



Novel blue and red electrochromic poly(azomethine ether)s based on electroactive triphenylamine moieties

Hung-Ju Yen, Guey-Sheng Liou *

Functional Polymeric Materials Laboratory, Institute of Polymer Science and Engineering, National Taiwan University, 1 Roosevelt Road, 4th Sec., Taipei 10617, Taiwan

ARTICLE INFO

Article history:

Received 18 September 2009

Received in revised form 22 October 2009

Accepted 3 November 2009

Available online 10 November 2009

Keywords:

Electrochemistry

Electrochromism

Polyethers

Azomethine

Triphenylamine

ABSTRACT

Two series of red and blue electrochromic aromatic poly(azomethine ether)s (PAMEs) containing electroactive triphenylamine (TPA) moieties in the backbone were prepared from the high-temperature polycondensation reactions of newly azomethine–triphenylamine (AM–TPA)-based biphenol monomers, 4,4'-di(4-hydroxybenzylideneamino)triphenylamine (**3**) and 4,4'-di(4-hydroxybenzylideneamino)-4''-methoxytriphenylamine (**4**), with difluoro compounds, respectively. The obtained polymers were readily soluble in many organic solvents and showed useful levels of thermal stability associated with high softening temperatures (215–240 °C) and high char yields (higher than 64% at 800 °C in nitrogen). In addition, the polymer films showed reversible electrochemical oxidation with high contrast ratio and unique anodic blue/red electrochromic behaviors.

© 2009 Elsevier B.V. All rights reserved.

1. Introduction

Electrochromic materials exhibited a reversible optical change in absorption or transmittance upon electrochemically oxidized or reduced, such as transition-metal oxides, inorganic coordination complexes, organic molecules, and conjugated polymers [1]. In general, the investigation of electrochromic materials had been directed towards optical changes in the visible region proved especially useful for variable reflectance mirrors, tunable windows, and electrochromic displays.

Poly(azomethine)s (PAMs) or poly(Schiff-base)s with aromatic backbones were considered as high performance polymers [2] due to their high thermal stability [3], excellent mechanical strength [4], and good optoelectronic properties [5]. In recent years, PAMs had also been ex-

plored for applications in organic electronics, such as light-emitting materials [6], pH sensors [7], and metal-collecting polymers [8]. However, their insolubility in common organic solvents limited their processability and application [9]. One of the common approaches for increasing the solubility and processability of PAMs without sacrificing high thermal stability was the introduction of various substituted aromatic ring into the polymer backbone [10], by using monomers with thiophene [11], phenylquinoxaline ring [12], cardo-structure [13], tetraphenylethene [14], and others [15]. Though PAMs made by vapor deposition of the monomers in a vacuum chamber have also been used as electron transporting layers in polymer light-emitting diodes [16], the preparation by solution-processable PAMs is beneficial for their fabrication of large-area, thin-film photonic devices.

The anodic oxidation pathway of electroactive TPA always associated noticeable color changed was well reported, and the electrogenerated TPA cation radical could be dimerized to form tetraphenylbenzidine (TPB), which

* Corresponding author.

E-mail address: gsliau@ntu.edu.tw (G.-S. Liou).

was more easily oxidized than the original TPA moieties [17]. Recently, we have reported some organo-soluble and high T_g aromatic polymers bearing TPA units in the main chain [18]. Because of the incorporation of bulky and three-dimensional TPA units along the polymer backbone, all the polymers were amorphous with good solubility in many aprotic solvents and exhibited excellent thin-film-forming capability.

In this contribution, we therefore synthesized the azomethine-triphenylamine (AM-TPA)-based aromatic poly(azomethine ether)s (PAMEs) from the new (AM-TPA)-based diol monomers, 4,4'-di(4-hydroxybenzylideneamino)-4''-triphenylamine (**3**) and 4,4'-di(4-hydroxybenzylideneamino)-4''-methoxytriphenylamine (**4**), with difluoro compounds, respectively. Incorporation of preformed TPA units into PAMEs allowed the retention of some of the favorable properties of polymers such as high thermal stability and glass transition temperature, whereas the ether linkages increase the solubility and enhance the film-forming ability. In addition to the general properties (such as inherent viscosities, solubility, and thermal properties), the electrochemical and electrochromic behaviors of these polymers were also investigated.

2. Experimental section

2.1. Materials

4,4'-Diaminotriphenylamine [19] (**1**) (mp: 186–187 °C), 4,4'-diamino-4''-methoxytriphenylamine [20] (**2**) (mp: 150–152 °C) and 2,5-bis(4-fluorophenyl)-1,3,4-oxadiazole [21] (**5b**) (mp: 205–206 °C) were synthesized according to a previously reported procedure. 4,4'-Difluoro-benzophenone (**5a**) (ACROS) was purified by recrystallization. Tetrabutylammonium perchlorate (TBAP) (ACROS) was recrystallized twice from ethyl acetate under a nitrogen atmosphere and then dried *in vacuo* prior to use. All other reagents were used as received from commercial sources.

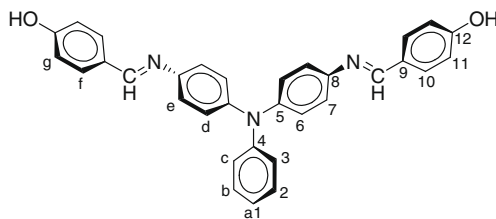
2.2. Monomer synthesis

The general procedure is as follows: To a solution of 30.10 mmol of diamino compound was stirred in 85 mL of ethanol and heated to 70 °C under nitrogen atmosphere. After the diamino compound was dissolved, 90.40 mmol of 4-hydroxybenzaldehyde was added and the mixture was then heated to reflux. After a further 15 h of reflux, the solution was cooled and poured slowly into 300 ml of stirred methanol, and the product was collected by filtration and dried *in vacuo* at 80 °C to give yellow powders.

2.2.1. 4,4'-Di(4-hydroxybenzylideneamino)triphenylamine (**3**)

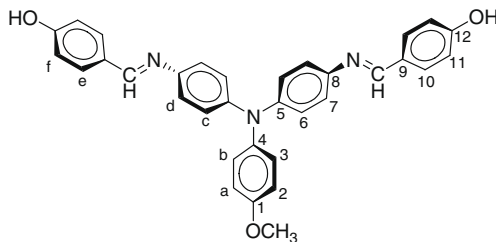
96.9 % in yield; mp of 259–260 °C (by DSC). ^1H NMR (300 MHz, DMSO- d_6 , δ , ppm): 6.87 (d, J = 8.4 Hz, 4H, H_f), 7.00–7.03 (m, 7H, $H_a + H_c + H_d$), 7.20 (d, J = 8.4 Hz, 4H,

H_e), 7.29 (t, J = 8.4 Hz, 2H, H_b), 7.75 (d, J = 8.4 Hz, 4H, H_g), 8.48 (s, 2H, $-\text{CH}=\text{N}-$), 10.09 (s, 2H, $-\text{OH}$). ^{13}C NMR (DMSO- d_6 , δ , ppm): 115.6 (C^{10}), 122.2 (C^7), 122.7 (C^1), 123.3 (C^3), 124.4 (C^6), 127.7 (C^5), 129.5 (C^2), 130.5 (C^{11}), 144.9 (C^8), 146.7 (C^9), 147.3 (C^4), 158.6 ($-\text{CH}=\text{N}-$), 160.4 (C^{12}). Anal. Calcd (%) for $\text{C}_{32}\text{H}_{25}\text{N}_3\text{O}_2$ (483.56): C, 79.48; H, 5.21; N, 8.69. Found: C, 79.34; H, 5.36; N, 8.55. ESI-MS: calcd for ($\text{C}_{32}\text{H}_{25}\text{N}_3\text{O}_2$) $^+$: m/z 483.6; found: m/z 482.6.



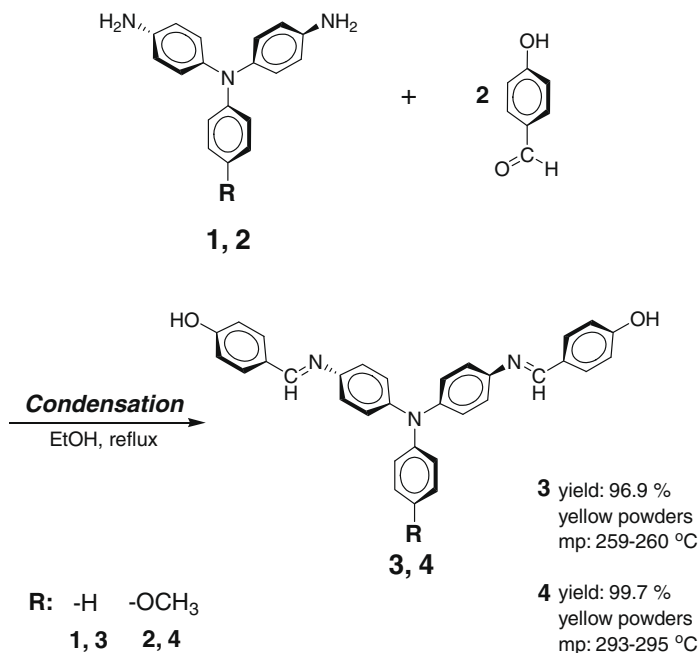
2.2.2. 4,4'-Di(4-hydroxybenzylideneamino)-4''-methoxytriphenylamine (**4**)

99.7 % in yield; mp of 293–295 °C (by DSC). ^1H NMR (300 MHz, DMSO- d_6 , δ , ppm): 3.73 (s, 3H, $-\text{OCH}_3$), 6.86 (d, J = 8.4 Hz, 4H, H_e), 6.91–6.96 (m, 6H, $H_a + H_c$), 7.04 (d, J = 8.4 Hz, 4H, H_d), 7.73 (d, J = 8.4 Hz, 4H, H_f), 8.46 (s, 2H, $-\text{CH}=\text{N}-$), 10.08 (s, 2H, $-\text{OH}$). ^{13}C NMR (DMSO- d_6 , δ , ppm): 55.3 ($-\text{OCH}_3$), 115.1 (C^2), 115.6 (C^{10}), 122.1 (C^7), 122.9 (C^6), 127.0 (C^3), 127.8 (C^5), 130.4 (C^{11}), 140.0 (C^4), 145.4 (C^8), 145.8 (C^9), 156.0 (C^1), 158.1 ($-\text{CH}=\text{N}-$), 160.4 (C^{12}). Anal. Calcd (%) for $\text{C}_{33}\text{H}_{27}\text{N}_3\text{O}_3$ (513.59): C, 77.17; H, 5.30; N, 8.18. Found: C, 77.15; H, 5.46; N, 8.15. ESI-MS: calcd for ($\text{C}_{33}\text{H}_{27}\text{N}_3\text{O}_3$) $^+$: m/z 513.6; found: m/z 512.6.



2.3. Polymer synthesis

The synthesis of PAME **1a** was used as an example to illustrate the general synthetic procedure. To a two necked 50 ml glass reactor was charged with diol monomer **3** (0.97 g, 2 mmol), **5a** (0.44 g, 2 mmol), and 4 ml *N*-methyl-2-pyrrolidinone (NMP), 2 ml of toluene, and an excess of potassium carbonate (0.41 g, 3 mmol). The reaction mixture was heated at 150 °C for 3 h to remove water during the formation of phenoxide anions, then heated at 170 °C for 1 h, 180 °C for 3 h, and finally heated at 190 °C for 1 h. After the reaction, the obtained polymer solution was poured slowly into 400 ml of acidified methanol/water ($v/v = 1/1$). The precipitate was collected by filtration, washed thoroughly with hot water and methanol, and dried under vacuum at 100 °C. Reprecipitations of the polymer by NMP/methanol were carried out twice for fur-



Scheme 1. Synthesis of AM-TPA-based diol monomers.

ther purification. The inherent viscosity of the obtained PAME **1a** was 0.20 dl/g (measured at a concentration of 0.5 g/dl in NMP at 30 °C). Anal. Calcd (%) of **1a** for (C₄₇H₃₇N₃O₃)_n: C, 81.60; H, 5.39; N, 6.07. Found:

C, 79.70; H, 5.61; N, 5.90. Anal. Calcd (%) of **1a** for (C₄₈H₃₉N₃O₄)_n: C, 79.87; H, 5.45; N, 5.82. Found: C, 77.97; H, 5.33; N, 5.89. The other PAMEs were prepared by an analogous procedure.

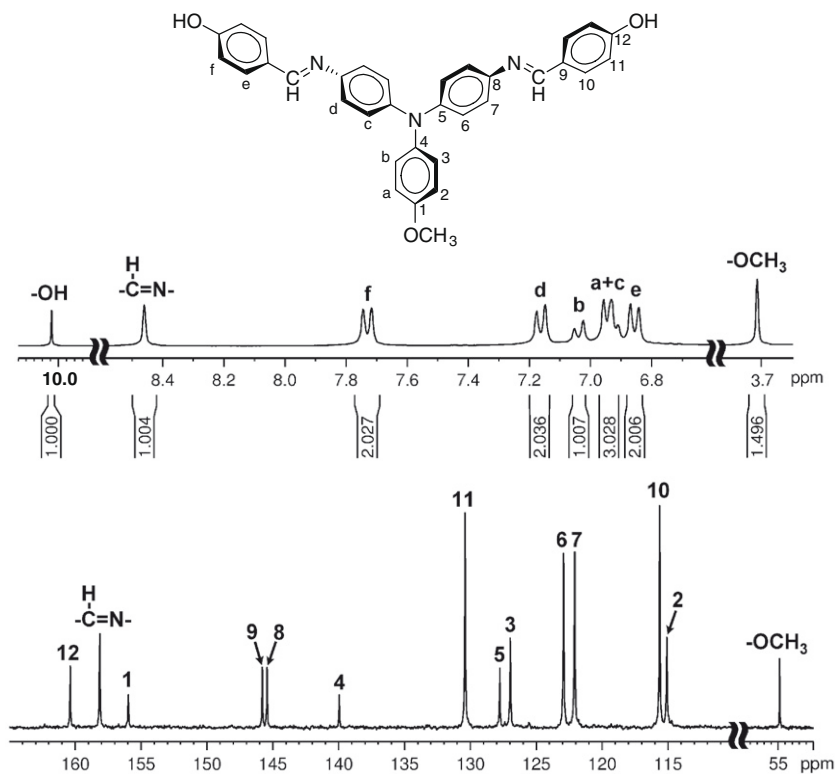


Fig. 1. ¹H NMR and ¹³C NMR spectra of diol monomer **4** in DMSO-*d*₆.

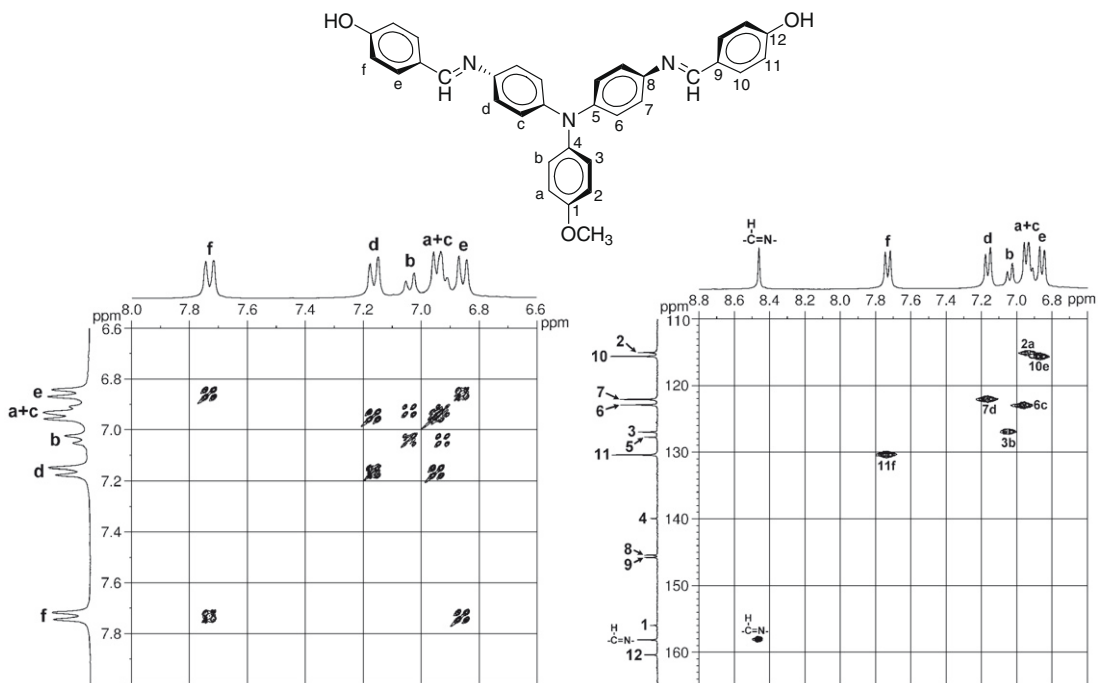
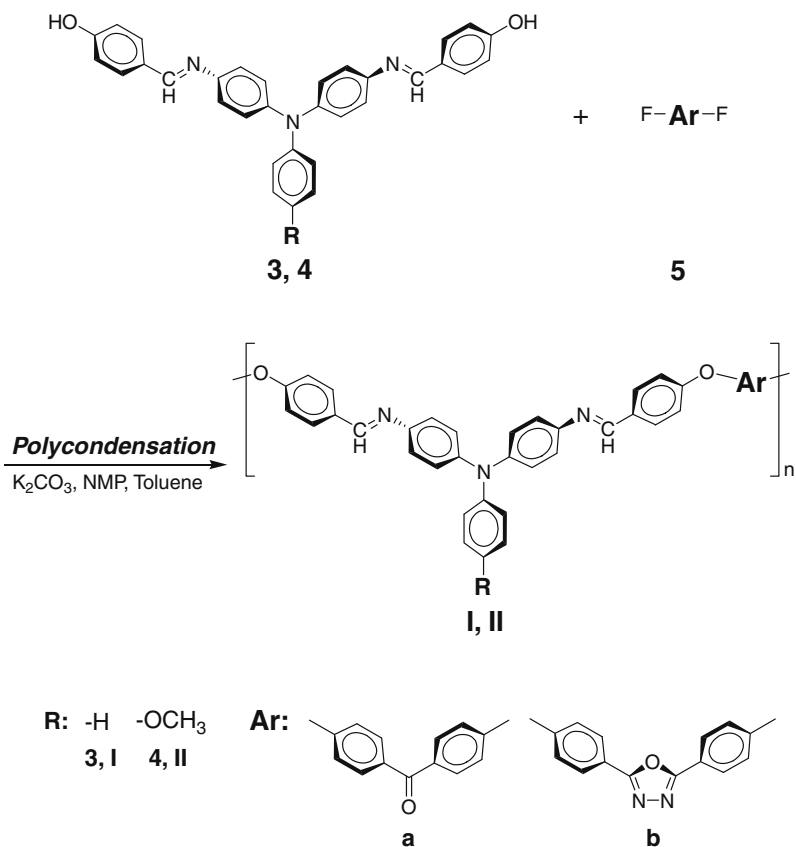


Fig. 2. H–H COSY and C–H HMQC spectra of diol monomer **4** in DMSO- d_6 .



Scheme 2. Synthesis of aromatic PAMEs.

2.4. Preparation of the poly(azomethine-ether) films

A solution of polymer was made by dissolving the poly-ether sample in NMP. The homogeneous solution was poured

into a glass Petri dish, which was placed in a 90 °C oven for 5 h to remove most of the solvent; then the semidried film was further dried *in vacuo* at 160 °C for 8 h. The obtained films were used for solubility tests and thermal analyses.

Table 1

Inherent viscosity^a and solubility behavior of PAMEs.

Polymer	η_{inh} (dl/g)	Solubility in various solvent ^b						
		NMP	DMAc	DMF	DMSO	<i>m</i> -cresol	THF	CHCl ₃
Ia	0.20	++	++	+–	+–	++	+–	+–
Ib	0.24	++	++	+–	+–	++	+–	+–
IIa	0.32	++	++	+–	+–	++	+–	+–
IIb	0.27	++	++	+–	+–	++	+–	+–

^a Measured at a polymer concentration of 0.5 g/dl in NMP at 30 °C.

^b The solubility was determined with a 2 mg sample in 2 ml of a solvent. ++, Soluble at room temperature; +, soluble on heating; +–, partially soluble or swelling; –, insoluble even on heating.

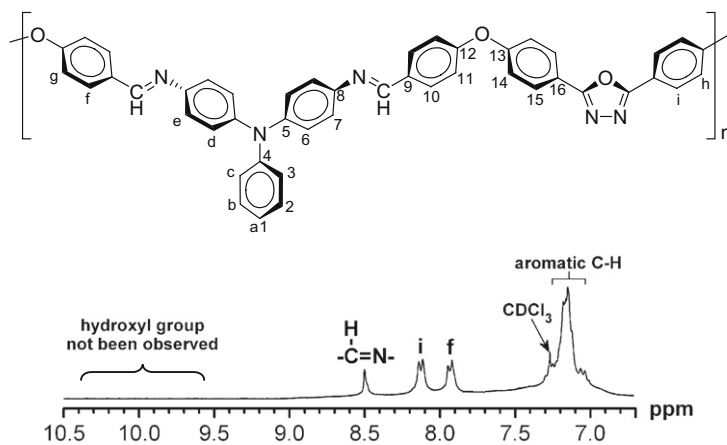


Fig. 3. ¹H NMR spectrum of PAME **Ib** in CDCl₃.

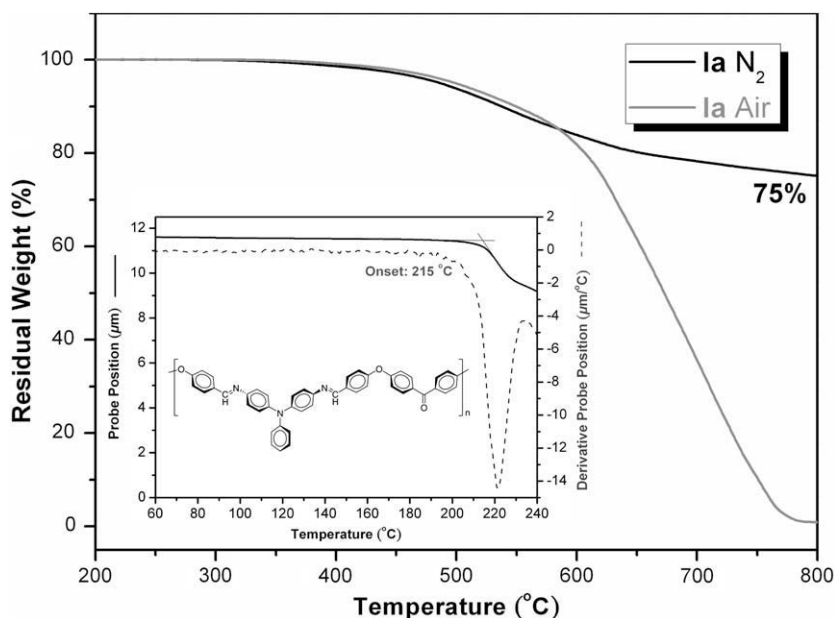


Fig. 4. TGA and TMA curves of PAME **Ia**.

Table 2
Thermal properties of PAMEs.

Polymer ^a	T_g (°C) ^b	T_d^5 (°C) ^c		T_d^{10} (°C) ^c		R_{w800} (%) ^d
		N ₂	Air	N ₂	Air	
Ia	215	490	500	540	550	75
Ib	219	480	480	510	515	68
IIa	227	460	475	505	525	64
IIb	240	450	460	485	495	65

^a The polymer film samples were heated at 300 °C for 1 h prior to all the thermal analyses.

^b Softening temperature measured by TMA with a constant applied load of 10 mN at a heating rate of 10 °C/min.

^c Temperature at which 5% and 10% weight loss occurred, respectively, recorded by TGA at a heating rate of 20 °C/min and a gas flow rate of 30 cm³/min.

^d Residual weight percentages at 800 °C under nitrogen flow.

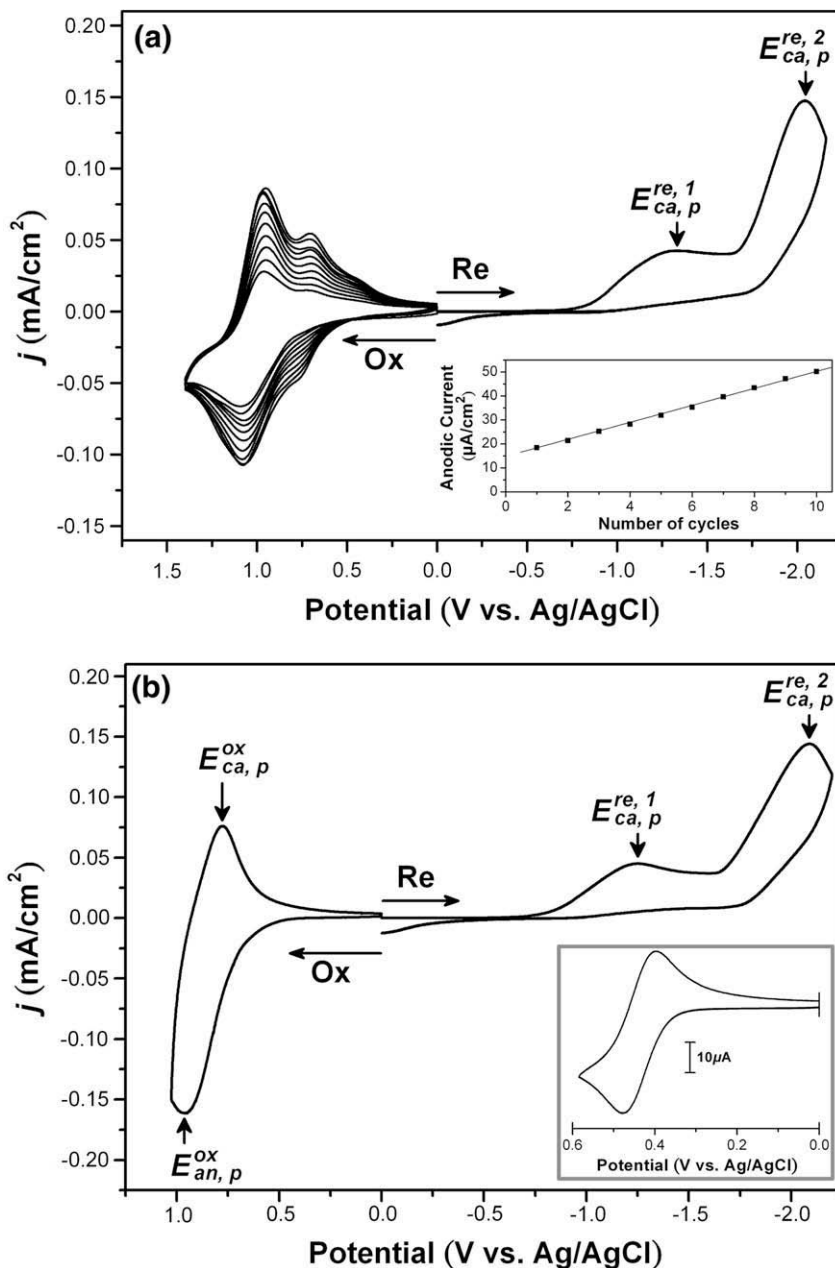
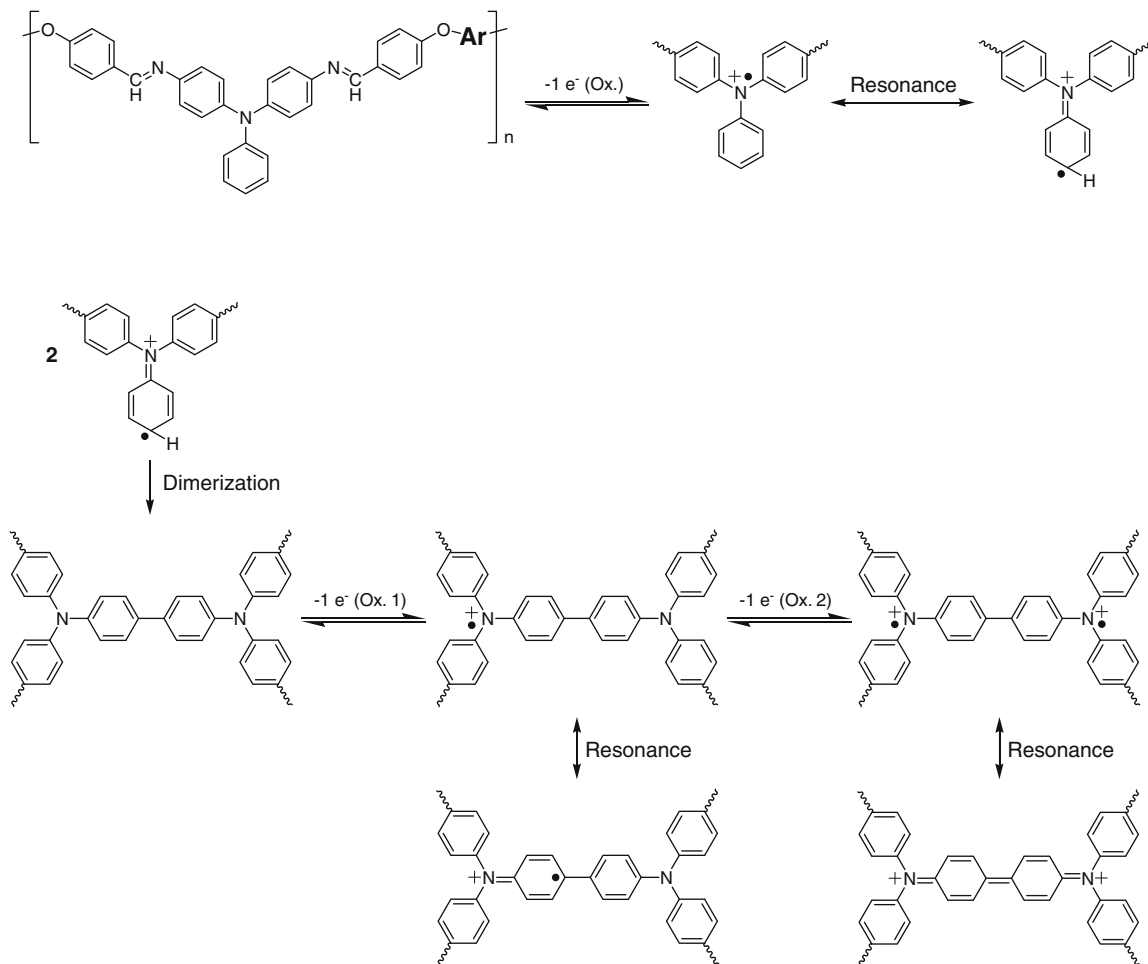


Fig. 5. Cyclic voltammogram of: (a) **Ia** and (b) **IIa** films on ITO-coated glass substrate in CH₃CN (oxidation) and DMF (reduction) solutions containing 0.1 M TBAP at scan rate of 50 and 100 mV/s, respectively. The inset showed a linear plot of the anodic current grown at 0.80 V vs. the number of scans and ferrocene, respectively.

2.5. Measurements

Elemental analyses were run in a Heraeus VarioEL-III CHNS elemental analyzer. Electrospray ionization (ESI) mass spectra were measured on LCQ Advantage mass spectrometer. NMR spectra were measured on a Bruker AC-300 MHz spectrometer in CDCl₃ and DMSO-*d*₆, and peak multiplicity was reported as follows: s, singlet; d, doublet; m, multiplet. The inherent viscosities were determined at

0.5 g/dl concentration using Tamson TV-2000 viscometer at 30 °C. Thermogravimetric analysis (TGA) was conducted with a PerkinElmer Pyris 1 TGA. Experiments were carried out on approximately 6–8 mg film samples heated in flowing nitrogen or air (flow rate = 20 cm³/min) at a heating rate of 20 °C/min. Softening temperatures (*T*_s) were taken as the onset temperatures of probe displacement on the TMA traces. Electrochemistry was performed with a CH Instruments 611B electrochemical analyzer. Voltammo-



Scheme 3. Proposed reaction for electropolymerization of PAME I.

Table 3

Redox potentials and energy levels of PAMES.

Index	Oxidation/V ^a		Reduction/V ^b			<i>E</i> _{HOMO} (eV) ^c	<i>E</i> _{LUMO} (eV) ^c	<i>E</i> _g (eV) ^d
	<i>E</i> _{1/2}	<i>E</i> _{onset}	<i>E</i> _{peak}		<i>E</i> _{onset}			
			1st	2nd				
Ia	1.03	0.82	-1.33	-2.04	-0.83	5.26	3.61	1.65
Ib	1.03	0.83	-1.31	-2.07	-0.79	5.27	3.65	1.62
IIa	0.87	0.70	-1.28	-2.06	-0.81	5.14	3.63	1.51
IIb	0.86	0.69	-1.27	-2.05	-0.77	5.13	3.67	1.46

^a From cyclic voltammograms vs. Ag/AgCl in CH₃CN. *E*_{1/2}: average potential of the redox couple peaks.

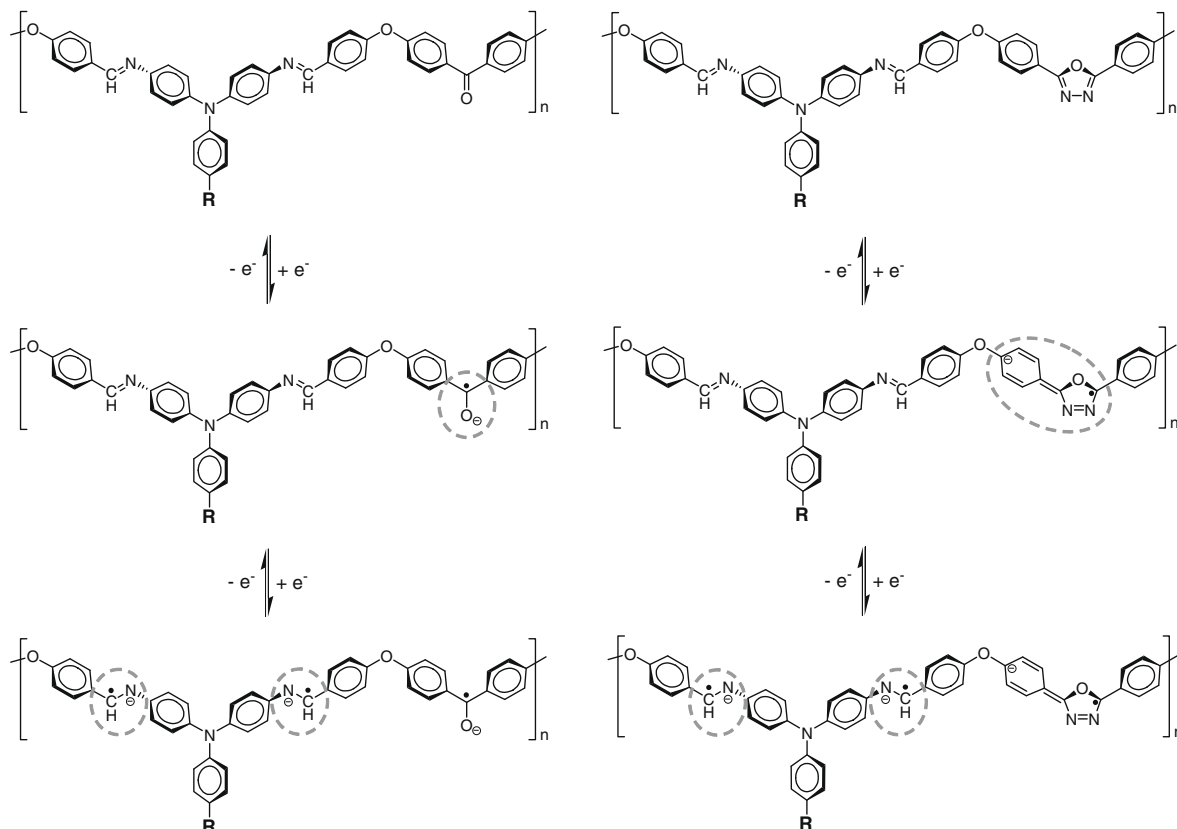
^b From cyclic voltammograms vs. Ag/AgCl in DMF.

^c The energy levels were calculated from cyclic voltammetry and were referenced to ferrocene (4.8 eV; onset = 0.36 V).

^d Difference between *E*_{HOMO} and *E*_{LUMO}.

grams were presented with the positive potential pointing to the left and with increasing anodic currents pointing downwards. Cyclic voltammetry (CV) was conducted with the use of a three-electrode cell in which ITO (polymer films area about 0.5 cm × 1.6 cm) was used as a working electrode. A platinum wire was used as an auxiliary electrode. All cell potentials were taken by using a homemade

Ag/AgCl, KCl (sat.) reference electrode. Spectroelectrochemical experiments were carried out in a cell built from a 1 cm commercial UV–visible cuvette using Hewlett–Packard 8453 UV–Visible diode array and Hitachi U-4100 UV–vis–NIR spectrophotometer. The ITO-coated glass slide was used as the working electrode, a platinum wire as the counter electrode, and Ag/AgCl cell as the reference elec-



Scheme 4. Mechanism of the electrochemical reduction for PAMes in an aprotic medium.

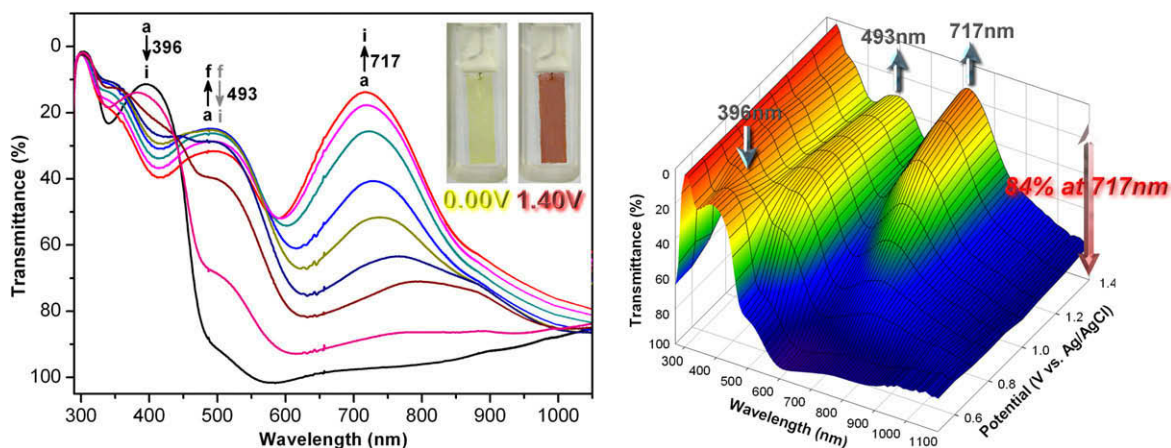


Fig. 6. Electrochromic behavior (left) at applied potentials of: (a) 0, (b) 0.60, (c) 0.70, (d) 0.80, (e) 0.90, (f) 1.00, (g) 1.10, (h) 1.25, (i) 1.40 (V vs. Ag/AgCl), and 3-D spectroelectrochemical behavior (right) from 0.50 to 1.40 (V vs. Ag/AgCl) of electropolymerized PAME **1a** thin film (~160 nm in thickness) on the ITO-coated glass substrate in 0.1 M TBAP/CH₃CN.

trode. The thickness of the PAME thin films was measured by alpha-step profilometer (Kosaka Lab., Surfcoorder ET3000, Japan). Colorimetry measurements were obtained using a Minolta CS-100A Chroma Meter. The color coordinates were expressed in the CIE 1931 Yxy color spaces.

3. Results and discussion

3.1. Monomer Synthesis

The new AM-TPA-based diol monomers **3** and **4** were synthesized by condensation reaction of the diamino compounds **1** and **2** with 4-hydroxybenzaldehyde, respectively (Scheme 1). Elemental analysis, MS, and NMR spectroscopic techniques were used to identify structures of the target diol monomers. Fig. 1 illustrates the ^1H NMR and ^{13}C NMR spectra of the diol monomer **4**. The ^1H and ^{13}C NMR chemical shift of $\text{CH}=\text{N}$ at 8.46 and 158.1 ppm, respectively, were consistent with the previous reports (Fig. 1) [6b,18d]. The ^1H NMR chemical shift of $\text{Ar}-\text{OH}$ shifts to low field at 10.08 ppm due to its acidity increased by the introduction of azomethine moiety. Assignments of each carbon and proton were assisted by the two-dimensional NMR spectra shown in Fig. 2, and these spectra agreed well with the proposed molecular structure.

3.2. Polymer synthesis

A series of newly TPA-based PAMEs were synthesized from the biphenol monomers **3** and **4** with corresponding difluoro compounds **5** (Scheme 2). The polymerization was carried out via potassium carbonate-mediated nucleophilic substitution reaction. All polymerization reactions proceeded homogeneously and the obtained PAMEs had inherent viscosities in the range of 0.20–0.32 dl/g (Table 1). All the polymers could afford transparent and tough films via solution casting implying the formation of polymers with high molecular weight. Typical ^1H NMR spectrum of PAME **1b** is illustrated in Fig. 3, and the hydroxyl group of

diol monomer around 10 ppm disappeared for PAMEs confirming the completion of polymerization.

3.3. Polymer properties

3.3.1. Basic characterization

The solubility behavior of the PAMEs was investigated qualitatively, and the results were also summarized in Table 1. The TPA-based PAMEs showed good solubility in polar organic solvents such as NMP, *N,N*-dimethylacetamide (DMAc), and *m*-cresol. The enhanced solubility made these polymers as potential candidates for practical applications by spin-coating or inkjet-printing processes to afford high performance thin films for optoelectronic devices.

The thermal properties of PAMEs were examined by TGA and TMA and the typical TGA and TMA curves of representative PAME **1a** were shown in Fig. 4, and the data were also listed in Table 2. All the prepared PAMEs exhibited good thermal stability with insignificant weight loss up to 400 °C under nitrogen or air atmosphere. The 10% weight loss temperatures of these polymers in nitrogen and air were recorded in the range of 485–540 and 495–550 °C, respectively. The concentration of carbonized residue (char yield) of these polymers in a nitrogen atmosphere was more than 64% at 800 °C. The high char yields of these polymers can be ascribed to their high aromatic content. The softening temperatures (T_s) of the polymer film samples were determined by the TMA method with a loaded penetration probe. They were obtained from the onset temperature of the probe displacement on the TMA traces and recorded in the range of 215–240 °C, depending upon the stiffness of the polymer chain.

3.3.2. Electrochemical properties

The electrochemical properties of the PAMEs were investigated by cyclic voltammetry (CV) conducted for the cast film on an indium–tin oxide (ITO)-coated glass substrate as working electrode in anhydrous CH_3CN and

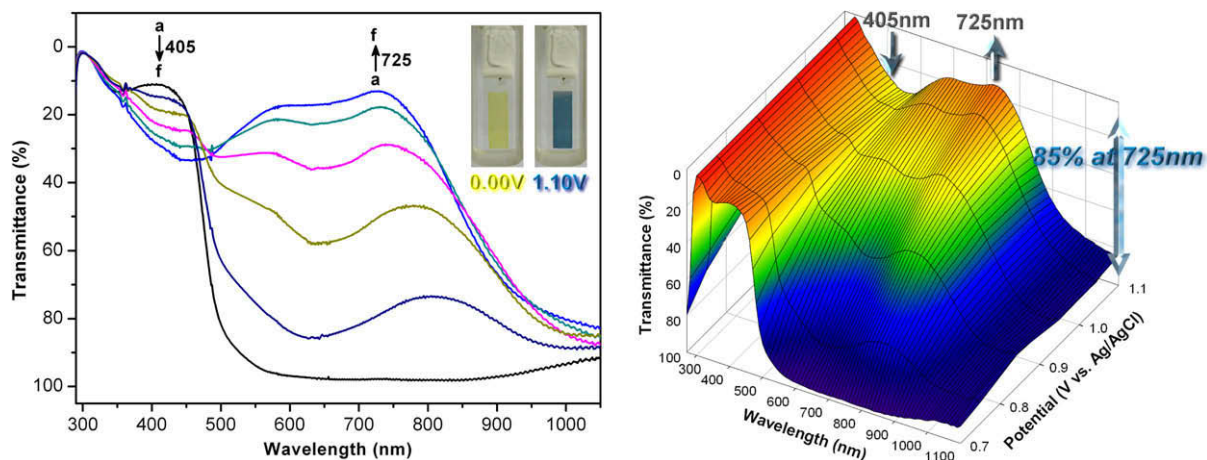
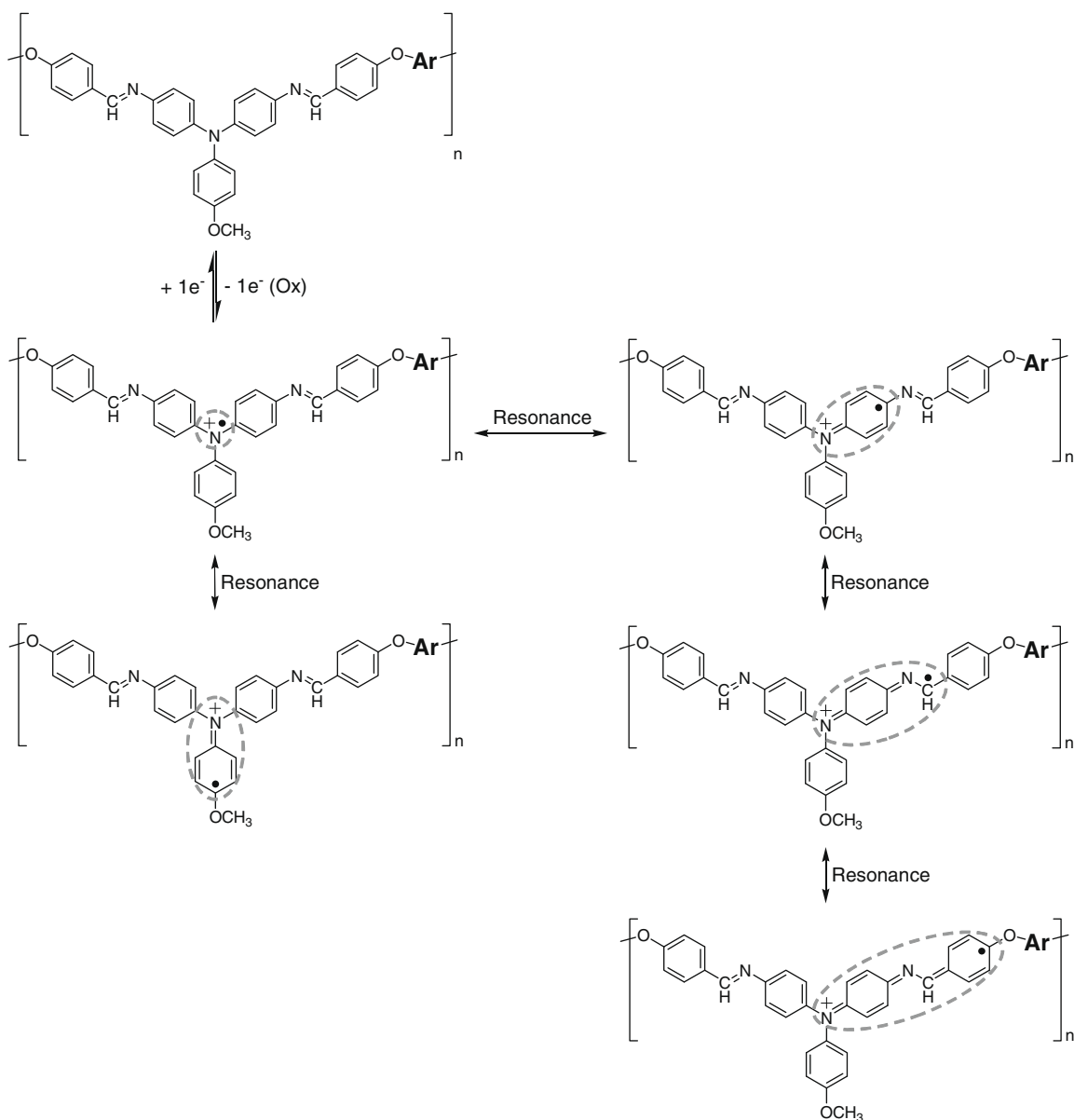


Fig. 7. Electrochromic behavior (left) at applied potentials of: (a) 0, (b) 0.75, (c) 0.85, (d) 0.95, (e) 1.05, (f) 1.10 (V vs. Ag/AgCl), and 3-D spectroelectrochemical behavior (right) from 0.70 to 1.10 (V vs. Ag/AgCl) of PAME **1a** thin film (~160 nm in thickness) on the ITO-coated glass substrate in 0.1 M TBAP/ CH_3CN .

DMF containing 0.1 M of TBAP as an electrolyte under nitrogen atmosphere for oxidation and reduction measurements, respectively. The typical CV for PAMEs **Ia** (without 4-methoxy-substituted) and **IIa** (with 4-methoxy-substituted) are shown in Fig. 5 for comparison, the results revealed one oxidation and two reduction processes for all the PAMEs. The PAME **IIa** (with 4-methoxy-substituted) exhibited lower oxidation potential than the corresponding **Ia** (without 4-methoxy-substituted) [20]. The cyclic voltammogram of PAME **Ia** indicated that TPA without 4-methoxy-substituted unit was irreversibly oxidized at applied potential range from 0 to 1.4 V upon repetitive scanning. A new pair of redox peaks corresponding to TPB was observed around 0.80 V from the second scan in Fig. 5a

indicating the TPB formation during oxidation of the TPA moieties of PAME **Ia** (Scheme 3). As shown in the inset of Fig. 5a, the plot of the anodic current at 0.80 V was linearly proportional to the number of scans confirming the occurrence of the oxidative coupling at the *para*-position of TPA in PAME **I** main chains. As summarized in Table 3, the reduction behavior of PAMEs **Ia**, **IIa** and **Ib**, **IIb** were attributed the methanone and oxadiazole groups in the polymer main chain, respectively. In addition, the second reduction stage around -2.05 V could be assigned to the imine ($\text{CH}=\text{N}$) groups in the polymer main chains [22], and the mechanism for the electrochemical reduction of PAMEs could be depicted as in Scheme 4. During the electrochemical oxidation scanning of the PAME thin films, the color of



Scheme 5. Mechanism of the electrochemical oxidation for PAMEs II.

the film changed from yellow to red and blue for PAMEs **I** and **II**, respectively. The redox potentials of the PAMEs as well as their respective highest occupied molecular orbital (HOMO) and lowest unoccupied molecular orbital (LUMO) (on the basis of ferrocene/ferrocenium is 4.8 eV below the vacuum level with $E_{\text{onset}} = 0.36$ V) estimated from the onset of their oxidation or reduction in CV experiments were summarized in Table 3.

3.3.3. Spectroelectrochemical and electrochromic properties

Spectroelectrochemical experiments were used to evaluate the optical properties of the electrochromic films. The PAME film was cast on an ITO-coated glass slide, and was placed in the optical path of the light beam from a UV–vis–NIR spectrophotometer, which allowed us to acquire electronic absorption spectra under potential control in a 0.1 M TBAP/MeCN solution. The UV–vis–NIR absorbance curves correlated to applied potentials and three-dimensional transmittance-wavelength-applied potential correlation of after-oxidized **Ia** film were depicted in Fig. 6. The strong absorption at around 396 nm, characteristic for the charge-transfer complex (CTC) formation between the electron-donating TPB group and the strongly electron-accepting AM group in the neutral form (0 V), decreased and new peaks at 493 and 717 nm grew up steadily upon electrochemical oxidation (increasing applied voltage from 0 to 1.00 V). The one-electron oxidation product, a stable monocation radical TPB, exhibited

absorption at 493 nm. As the anodic potential higher than 1.00 V, the absorption peak at 717 nm corresponding to the formation of a dication of TPB unit grew up. From the inset shown in Fig. 6, the PAME **Ia** film switched from a transmissive neutral state (light-yellow; Y: 74; x, 0.372; y, 0.444) to a highly absorbing oxidized state (red; Y: 13; x, 0.601; y, 0.351) with an high optical transmittance change ($\Delta\%$) of 84%.

On the other hand, the spectroelectrochemical behavior of PAME **Ila** film shown in Fig. 7 also exhibited strong absorption at around 405 nm in the neutral form (0 V). Upon oxidation (increasing applied voltage from 0 to 1.10 V), the intensity of the absorption peak at 405 nm decreased while a new peak at 725 nm gradually increased in intensity due to the formation of a stable monocation radical of the AM-TPA unit. Furthermore, the broadened absorbance band was because of the monocation radical of AM-TPA unit having more extended conjugation length than TPA (Scheme 5), which resulted different and unique coloration from other TPA-based electrochromic materials [20,23]. From the inset shown in Fig. 7, the PAME **Ila** film switches from a transmissive neutral state (light-yellow; Y: 70; x, 0.374; y, 0.453) to a highly absorbing oxidized state (blue; Y: 10; x, 0.246; y, 0.305) with an high optical transmittance change ($\Delta\%$) of 85% at 725 nm. Besides, the distribution of coloration across these polymer films was very homogeneous with high electrochemical stability.

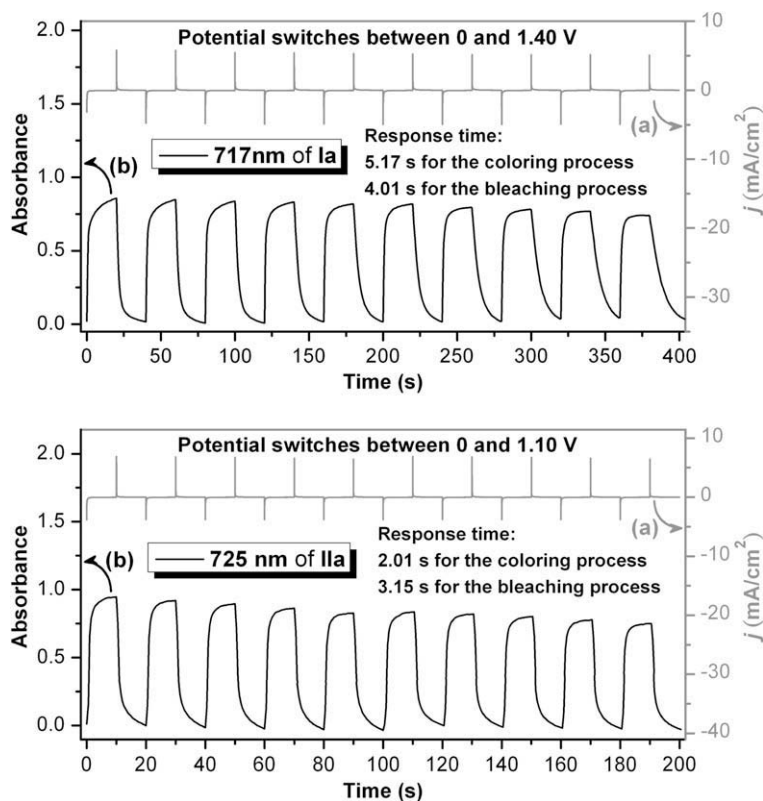


Fig. 8. (a) Current consumption and (b) electrochromic switching and absorbance change monitored for PAME thin films (~160 nm in thickness) on the ITO-coated glass substrate (coated area: 1.6 cm × 0.5 cm) in 0.1 M TBAP/CH₃CN.

For electrochromic switching studies, polymer films were cast on ITO-coated glass slides in the same manner as described above, and chronoamperometric and absorbance measurements were performed. While the films were switched, the absorbance at the given wavelength was monitored as a function of time with UV–vis–NIR spectroscopy (Fig. 8). The switching time was calculated at 90% of the full switch because it is difficult to perceive any further color change with naked eye beyond this point. The electrochromic coloration efficiency ($\eta = \delta OD/Q$) of PAMes **Ia** and **Ila** are calculated as 162 and 195 cm²/C, respectively [18j]. After several coloring/bleaching cyclic scans, the polymer films still exhibited good stability of electrochromic characteristics.

4. Conclusion

Two series of blue and red electrochromic aromatic PAMes containing electroactive TPA moieties in the backbone were prepared from the potassium carbonate-mediated nucleophilic substitution reaction of newly azomethine–triphenylamine (AM–TPA)-based biphenol monomers with difluoro compounds. Introduction of electron-donating TPA groups to the polymer main chain not only afford high T_g and good thermal stability but also leads to good solubility of the PAMes. All the obtained polymers revealed valuable electrochromic characteristics such as high contrast in visible region and unique blue/red electrochromic behavior, indicating the incorporation of azomethine groups into TPA-based polymers is a new approach for tuning the coloration changed.

Acknowledgement

The authors are grateful to the National Science Council of the Republic of China for its financial support of this work.

References

- [1] (a) P.M.S. Monk, R.J. Mortimer, D.R. Rosseinsky, *Electrochromism: Fundamentals and Applications*, VCH, Weinheim, Germany, 1995; (b) R.J. Mortimer, *Chem. Soc. Rev.* 26 (1997) 147–156; (c) D.R. Rosseinsky, R.J. Mortimer, *Adv. Mater.* 13 (2001) 783–793; (d) S. Liu, D.G. Kurth, H. Mohwald, D. Volkmer, *Adv. Mater.* 14 (2002) 225–228; (e) T. Zhang, S. Liu, D.G. Kurth, C.F.J. Faul, *Adv. Funct. Mater.* 19 (2009) 642–652; (f) A. Maier, A.R. Rabindranath, B. Tiede, *Adv. Mater.* 21 (2009) 959–963.
- [2] C.J. Yang, S.A. Jenekhe, *Chem. Mater.* 3 (1991) 878–887.
- [3] I.K. Spiliopoulos, J.A. Mikroyannidis, *Macromolecules* 29 (1996) 5313–5319.
- [4] P. Cerrada, L. Oriol, M. Pinol, J.L. Serrano, I. Iribarren, S. Munoz Guerra, *Macromolecules* 29 (1996) 2515–2523.
- [5] (a) N. Kiriy, V. Bocharova, A. Kiriy, M. Stamm, F.C. Krebs, H.J. Adler, *Chem. Mater.* 16 (2004) 4765–4771; (b) G. Zotti, A. Randi, S. Destri, W. Porzio, G. Schiavon, *Chem. Mater.* 14 (2002) 4550–4557.
- [6] (a) A. Kimoto, K. Masachika, J.S. Cho, M. Higuchi, K. Yamamoto, *Chem. Mater.* 16 (2004) 5706–5712; (b) D. Sek, A. Iwan, B. Jarzabek, B. Kaczmarczyk, J. Kasperczyk, Z. Mazurak, M. Domanski, K. Karon, M. Lapkowski, *Macromolecules* 41 (2008) 6653–6663.
- [7] M.K. Choi, H.L. Kim, D.H. Suh, *J. Appl. Polym. Sci.* 101 (2006) 1228–1233.
- [8] (a) M. Cazacu, M. Marcu, A. Vlad, A. Tóth, C. Racles, *J. Polym. Sci. Part A: Polym. Chem.* 41 (2003) 3169–3179; (b) J.M. Adell, M.P. Alonso, J. Barberá, L. Oriol, M. Piñol, J.L. Serrano, *Polymer* 44 (2003) 7829–7841.
- [9] (a) H.H. Yang, *Aromatic High Strength Fibers*, Wiley, New York, 1989; (b) H.R. Kricheldorf, G. Schwarz, *Handbook of Polymer Synthesis, Part B*, in: H.R. Kricheldorf (Ed.), Dekker, New York, 1992, pp. 1673–1684.
- [10] T. Yamamoto, Z.H. Zhou, T. Kanbara, M. Shimura, K. Kizu, T. Maruyama, Y. Nakamura, T. Fukuda, B.L. Lee, N. Ooba, S. Tomaru, T. Kurihara, T. Kaino, K. Kubota, S. Sasaki, *J. Am. Chem. Soc.* 118 (1996) 10389–10399.
- [11] (a) C. Wang, S. Shieh, E. LeGoff, M.G. Kanatzidis, *Macromolecules* 29 (1996) 3147–3156; (b) O. Thomas, O. Inganas, M.R. Anderson, *Macromolecules* 31 (1998) 2676–2678.
- [12] D.J. Klein, D.A. Modarelli, F.W. Harris, *Macromolecules* 34 (2001) 2427–2437.
- [13] C.L. Chiang, C.F. Shu, *Chem. Mater.* 14 (2002) 682–687.
- [14] T. Matsumoto, F. Yamada, T. Kurosaki, *Macromolecules* 30 (1997) 3547–3552.
- [15] N. Giuseppone, G. Fuks, J.M. Lehn, *Chem. Eur. J.* 12 (2006) 1723–1735.
- [16] (a) W. Fischer, F. Stelzer, F. Meghdadi, G. Leising, *Synth. Met.* 76 (1996) 201–204; (b) M.S. Weaver, D.D.C. Bradley, *Synth. Met.* 83 (1996) 61–66.
- [17] (a) T. Zhang, B. Toth, *Anal. Chem.* 72 (2000) 2533–2540; (b) M. Oyama, K. Nozaki, S. Okazaki, *Anal. Chem.* 63 (1991) 1387–1392; (c) S.C. Creason, J. Wheeler, R.F. Nelson, *J. Org. Chem.* 37 (1972) 4440–4446; (d) E.T. Seo, R.F. Nelson, J.M. Fritsch, L.S. Marcoux, D.W. Leedy, R.N. Adams, *J. Am. Chem. Soc.* 88 (1966) 3498–3503.
- [18] (a) S.H. Cheng, S.H. Hsiao, T.H. Su, G.S. Liou, *Macromolecules* 38 (2005) 307–316; (b) G.S. Liou, S.H. Hsiao, N.K. Huang, Y.L. Yang, *Macromolecules* 39 (2006) 5337–5346; (c) G.S. Liou, S.H. Hsiao, W.C. Chen, H.J. Yen, *Macromolecules* 39 (2006) 6036–6045; (d) G.S. Liou, H.Y. Lin, Y.L. Hsieh, Y.L. Yang, *J. Polym. Sci. Part A: Polym. Chem.* 45 (2007) 4921–4932; (e) G.S. Liou, C.W. Chang, *Macromolecules* 41 (2008) 1667–1674; (f) S.H. Hsiao, G.S. Liou, Y.C. Kung, H.J. Yen, *Macromolecules* 41 (2008) 2800–2808; (g) C.W. Chang, C.H. Chung, G.S. Liou, *Macromolecules* 41 (2008) 8441–8451; (h) C.W. Chang, H.J. Yen, K.Y. Huang, J.M. Yeh, G.S. Liou, *J. Polym. Sci. Part A: Polym. Chem.* 46 (2008) 7937–7949; (i) G.S. Liou, H.J. Yen, M.C. Chiang, *J. Polym. Sci. Part A: Polym. Chem.* 47 (2009) 5378–5385; (j) H.J. Yen, G.S. Liou, *Chem. Mater.* 21 (2009) 4062–4070.
- [19] Y. Oishi, H. Takado, M. Yoneyama, M. Kakimoto, Y. Imai, *J. Polym. Sci. Part A: Polym. Chem.* 28 (1990) 1763–1769.
- [20] C.W. Chang, G.S. Liou, S.H. Hsiao, *J. Mater. Chem.* 17 (2007) 1007–1015.
- [21] J.L. Hedrick, R. Twieg, *Macromolecules* 25 (1992) 2021–2025.
- [22] İ. Kaya, S. Koyuncu, S. Çulhaoglu, *Polymer* 49 (2008) 703–714.
- [23] T.X. Su, S.H. Hsiao, G.S. Liou, *J. Polym. Sci. Part A: Polym. Chem.* 43 (2005) 2085–2098.